

NiO–Al₂O₃ catalysts prepared at high pH variation of structure and texture upon thermal treatment

M. N. RAMSIS, E. R. SOUAYA, M. ABD-EL-KHALIK and S. A. SELIM*
Department of Chemistry, Faculty of Science, Ain Shams University, Abbassia, Cairo, Egypt

A series of five catalysts of NiO–Al₂O₃ of varying content (IA–VA) were prepared at pH ~ 10 and dried at 80° C using neutral mesoporous alumina composed of γ -Al₂O₃ and poorly crystalline boehmite. Structural changes produced upon heat treatment up to 700° C were followed using XRD, TG and DTA techniques. The surface texture of the samples was investigated by nitrogen adsorption at 77 K. The effect of soaking period on the resulting preparation and on its thermally treated products was also investigated (III Aa).

The presence of nickel in the form of the amine complex had a marked effect on the crystallinity of the support changing the boehmite to the well crystalline form—an effect which was not observed in the absence of the nickel amine complex. The presence of NH₃ alone in the medium resulted in the appearance of two broad bands covering d distance ranges of 0.545 to 0.521 nm and 0.432 to 0.386 nm that also appeared in the XRD patterns of the catalyst samples. The ammonia penetrates between the layer structure of the support thus changing its interlayer distance.

Soaking for 7 days was found to represent non-equilibrium conditions compared to soaking for 15 days.

NiAl₂O₃ was characterized in the catalyst samples and NiO appeared in samples heated at 225° C and increased at 325° C resulting from the decomposition of the physically adsorbed surface species [Ni(NH₃)₆](NO₃)₂ and [Ni(NH₃)₆](OH)₂, respectively. The latter became pronounced for higher nickel concentrations as observed from DTA and DTG. The former decomposes exothermally at around 260° C and the latter endothermally at 325° C after losing the NH₃ ligand in the temperature range 245 to 265° C.

At nickel contents greater than 4.6% and at temperatures greater than 225° C a surface compound appeared with characteristic d distances in the ranges 0.202 to 0.2034 nm and 0.2363 to 0.2348 nm depending on treatment temperature. It results from the attack of the nickel amine complex on two adjacent hydroxyl groups.

An increase in the surface parameters of Al₂O₃ was observed upon soaking in NH₄OH solution alone and from pore analysis is found to contain two groups of mesopore sizes. The presence of the least amount of nickel content (1.5%) produced a marked increase in both specific area and total pore volume accompanied by a decrease in average pore radius. These changes reflect the structural changes of the support observed upon impregnation in the nickel–amine complex. Variations of the surface parameters of the catalyst samples with further increase in nickel content depend on the nickel species formed. However, at a nickel content of 9.6% more pores are being exposed that result from the penetration of more nickel ions between the support particulates. At still higher nickel contents blocking of the narrower pores and narrowing of the wider pores occurs as their V_t-t plots indicate. Despite this narrowing the catalyst samples are still predominantly mesoporous retaining, in most cases the existence of two groups of pore sizes.

Variations in soaking period seems to affect the texture of the low temperature samples but for samples treated at temperatures above 500° C the surface parameters are comparable irrespective of the period of soaking.

*To whom correspondence should be addressed.

1. Introduction

Transition metal ions carried on porous supports are widely used for the preparation of active catalysts. The nature of the introduced metal cations whether simple or in a complex form—at the initial stages of preparation—contribute markedly to the activity of the resulting catalyst [1–6].

These metal ions are either ion exchanged with a surface site [7–11] or merely physically adsorbed and may or may not react with the support upon thermal treatment. Accordingly the nature of both the surface support—for providing these surface sites—and the ionic species of the transition metal ions are significant for the production of highly active catalysts.

Among the various supports commonly used alumina is found to supply a heterogenous surface suitable for adsorption and catalysis [12–16]. An insight to the nature of the various sites at the surface was given by a model proposed by Peri [12].

Nickel ions—in the form of the amine complex—have previously been supported on silica whereby a surface silicate was found to form upon drying at 80°C [17]. Alumina was used in an extension of the work to follow the formation of such new surface compounds besides investigating the role of impregnation period.

A detailed thermal and structural study of a series of catalyst preparations with various nickel contents is given here. Techniques such as XRD, DTA, TG (and DTG) are employed.

The variations in the textural characteristics accompanying the impregnation of the complex metal ions are also investigated using low temperature nitrogen adsorption.

2. Experimental details

2.1. Materials

The alumina used as support is a product (neutral) originally produced for chromatographic adsorption analysis (according to Brockman (II) Reanal-Hungary).

A series of five catalysts (IA–VA) with different nickel contents was prepared by soaking 30 g of the alumina support in a solution of nickel–amine complex of the required concentration. The complex was prepared by dissolving the calculated weight of $\text{Ni}(\text{NO}_3)_2 \cdot 6\text{H}_2\text{O}$ (BDH) in 100 ml H_2O and the amine complex formed by adding conc. NH_4OH solution

with constant stirring until the precipitate disappeared and the total volume of liquid was made up to 200 ml. The admixtures were then allowed to stand for 15 days at room temperature, then filtered and dried at 80°C overnight. Sample IIIAa was prepared similarly to IIIA but soaked for a period of 7 days to study the effect of the soaking period. It was filtered and dried as before.

In all cases the pH dropped from ~ 11 to ~ 10 upon soaking. Thermally treated products were obtained for all samples in the temperature range 120 to 700°C after 2 h in static air. In the following sections the treatment temperature is given after the sample designation.

2.2. Methods

The nickel content estimated as NiO, was obtained through the analysis of the impregnating solution before and after soaking of the alumina, using EDTA titrant. The results are given in Table I, column 2.

XRD patterns were obtained using a Philips X-Ray diffraction model pw 1050/70 and iron filtered cobalt radiation. The d distances were calculated and compared with their relative intensities with data in the ASTM cards [18, 19].

Thermogravimetric analysis was carried out in the presence of static air at a heating rate of $10^\circ\text{C min}^{-1}$ using a Stanton–Redcroft thermobalance type 750/770 connected to a Kipp and Zonnen BD9—a two-channel automatic recorder.

Differential thermal analysis curves were recorded using α -alumina as an inert standard using a Stanton Redcroft STA 780 apparatus with a linear rate of heating of $10^\circ\text{C min}^{-1}$. IR spectra, whenever required, were measured with a Pye-Unicam SP3-200 A spectrograph using KBr pellets.

Adsorption–desorption isotherms of purified nitrogen at 77 K were determined using a conventional volumetric apparatus.

3. Results and discussion

3.1. Structural characteristics

3.1.1. X-Ray

The X-ray analysis of the pure alumina used as support showed it to be mainly composed of γ -alumina and poorly crystalline boehmite together with traces of κ -alumina. The XRD patterns of the catalyst samples IA–IVA and IIIAa exhibit some broad diffraction bands, the tops of which indicate the presence of ill

TABLE I Chemical and thermogravimetric analysis data for the investigated catalyst samples

Catalyst Sample	Ni Content (% NiO)	Loss in weight				
		First step (%)	Second step (%)	Third step < 400°C (%)	Last step (%)	Total (%)
IA	1.5	2.4	1.8	3.5	1.1	7.6
IIA	3.2	3.1	2.3	3.6	1.0	9.1
IIIA	4.6	3.1	2.3	4.2	1.0	9.6
IIIAa	4.3	2.4	1.8	4.7	1.0	8.9
IVA	9.6	2.9	2.4	4.9	1.0	10.2
VA	13.4	3.1	2.3	5.9	0.9	11.3
Al_2O_3 (Soaked in water)	–	2.3	–	3.9 (one step)	1.1	7.3

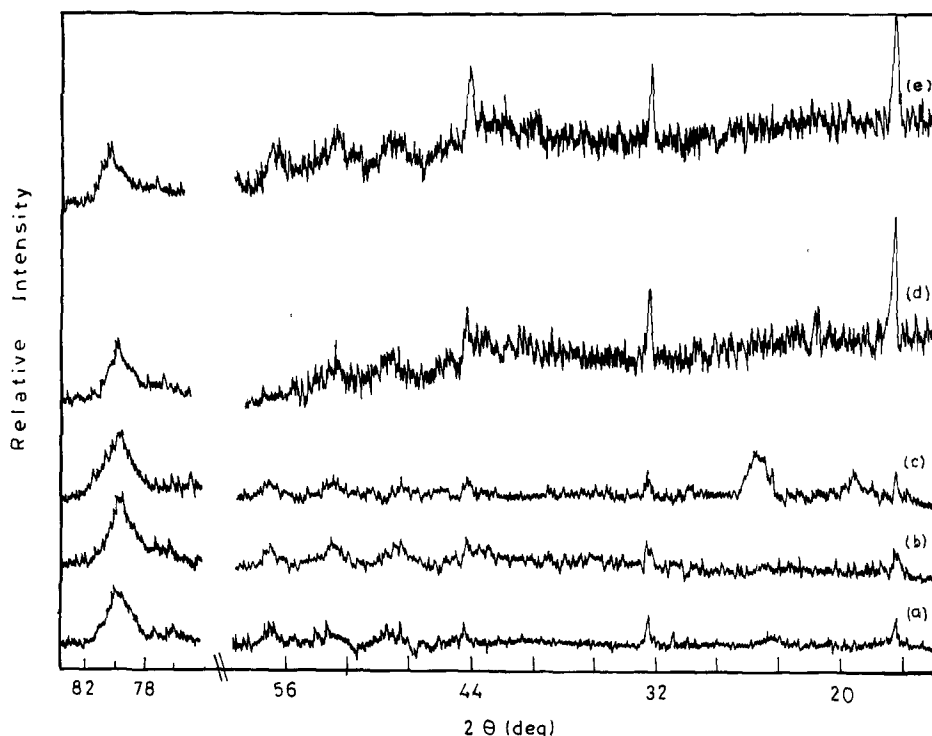


Figure 1 XRD patterns of the alumina support soaked in: (a) water (b) NaOH solution (c) NH_4OH solution and catalyst samples (d) IA and (e) IVA.

defined NiAl_2O_4 [18] together with the bands characterizing the support where the intensity and crystallinity of boehmite has markedly increased (d distances of 0.6112, 0.316 and 0.2343 nm). This observed increase in the crystallinity and intensity of boehmite could arise either from the soaking in the high pH medium (alkaline medium) [20] and/or the presence of the nickel ions at such pH may have a role in producing the observed effect. To distinguish the major contributing factor, two alumina samples were tested, one placed in ammonia solution and the other in sodium hydroxide solution, both at the same pH and for the same duration as the catalyst samples, then filtered and dried at 80°C . The intensity and crystallinity of the bands characterizing boehmite increased only slightly as compared to the catalyst samples themselves. It is slightly more pronounced for NaOH than for NH_4OH . (Fig. 1). In cases of the alumina sample soaked in NH_4OH solution, two new broad bands covering d distance ranges of 0.554 to 0.5215 nm and 0.423 to 0.386 nm that also appeared in the catalyst samples but not in the sample soaked in NaOH which clearly shows it does not result from a hydrated or hydroxylated species. It thus seems reasonable to believe that the ammonia molecules penetrate between the layer structure of the alumina thus changing the interlayer distance and giving rise to the observed X-ray bands. Soaking the support in the nickel complex solution at such a high pH of ~ 10 and for a long period (15 days) followed by treatment at 80°C seems suitable to convert gelatinous boehmite to the crystalline form. We therefore believe that the presence of nickel ions is responsible for the observed changes in intensity and crystallinity of boehmite as will be soon discussed.

The XRD pattern of the sample soaked for 7 days did not show any significant differences in the XRD pattern to that soaked for 15 days.

The intensity of the bands characterizing the

NiAl_2O_4 increases slightly with an increase in nickel content. Typical X-ray patterns of samples IA and IVA are shown in Fig. 1.

The formation of nickel aluminate under the present experimental conditions is quite feasible. Soaking the alumina support at such high pH brings about its dissolution, being amphoteric in nature, with the formation of $[\text{Al}(\text{OH})_4]^-$ (aq) or $[\text{Al}(\text{H}_2\text{O})_2(\text{OH})_4]^-$ [21] (assuming the coordination number of aluminium to be 6). In the presence of $[\text{Ni}(\text{NH}_3)_6]^{2+}$ ions, NiAl_2O_4 can thus be easily formed. As $\gamma\text{-Al}_2\text{O}_3$ has a defect spinel structure, so boehmite may also be related; the alumina support supplies a suitable substrate for NiAl_2O_4 to form and grow on it. Meanwhile it is worth considering the possibility of Ni^{2+} ions penetrating the alumina lattice [22] (after being stripped from the ammonia ligand) to occupy the vacant cation sites ($\text{Al}_{21}^{\text{III}}\square_{25}\text{O}_{32}$) [23] as the presence of the nickel ions seems essential for the changes observed in the crystallinity of boehmite. There is a controversy over whether these vacancies are in the octahedral [23, 24] or tetrahedral [25] positions. Whichever position the Ni^{2+} ions occupy, it appears that the crystal geometry of the support is stabilized and improved when the occupation is limited. Such a penetration, if it occurs in an appropriate proportion to the aluminium in the lattice of the unit cell, may also result in the formation of a spinel.

However, it is still not clear whether the increase in crystallinity of boehmite results from the penetration of nickel ions into the lattice in amounts below that required for spinel formation or that the adsorption on the support surface of the spinel from the solution causes the alumina to acquire a more organized lattice structure.

Meanwhile NiAl_2O_4 usually does not follow the normal spinel structure where the nickel should occupy the tetrahedral and the aluminium the octahedral sites. As the crystal field stabilization energy of Ni^{2+} is

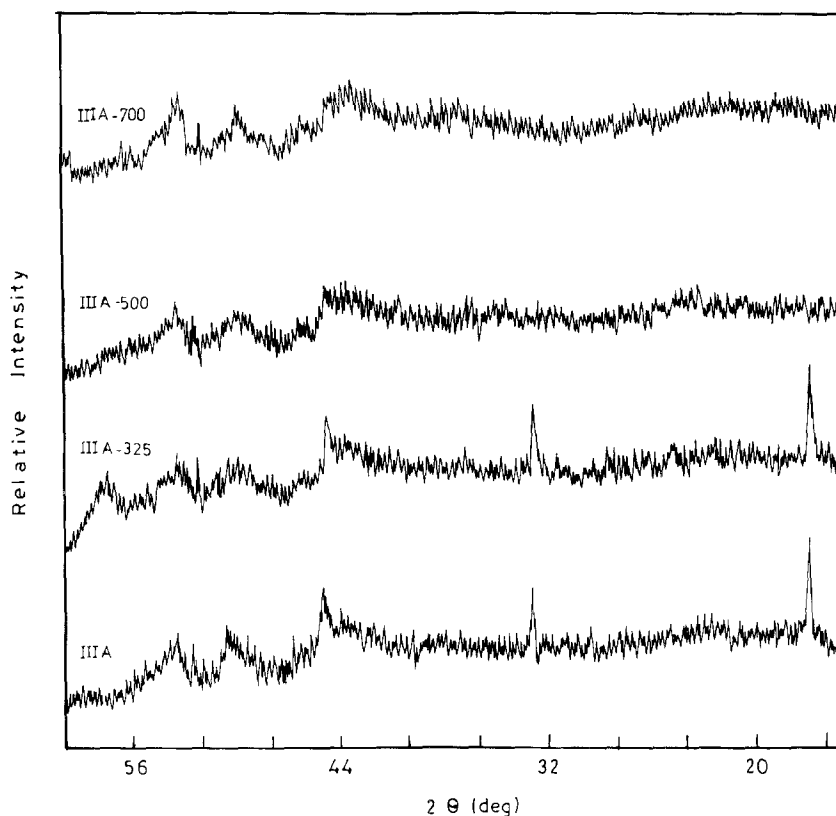


Figure 2 XRD patterns of sample IIIA and its thermally treated products.

greater in octahedral than in tetrahedral coordination, this makes the normal and inverse structures almost equal in energy and there is almost complete normalization of all cations on all the available sites [21]. This results in a defect spinel structure, as all crystallographically identical sites within the unit cell are not occupied by the same cation. If such a spinel is formed it will probably be in the surface layers only of the support.

Thermal treatment at 225 and 325°C affects the surface species markedly (Fig. 2). NiO starts to appear for samples heated at 225°C at all nickel concentrations, but the intensity of the peaks is relatively increased by heating at 325°C. It should be noted that the intensity of the peaks of the support itself markedly exceeds those of the supported nickel compounds. DTG data (given later in Fig. 4) show a loss at about 325°C which is preceded by a loss at about 270°C. The simultaneous appearance of NiO at such temperatures clearly points to the decomposition of some adsorbed species. Two physically adsorbed species are believed to exist on the surface sites, namely, $[\text{Ni}(\text{NH}_3)_6](\text{NO}_3)_2$ and $[\text{Ni}(\text{NH}_3)_6](\text{OH})_2$, the former decomposes exothermally (see Section 3.1.3.) in the temperature range 240 to 270°C and the latter endothermally at about 325°C after the evolution of the ammonia ligand at lower temperatures probably also at 240 to 270°C.

The main band of $\text{Ni}(\text{OH})_2$ occurring at 0.233 nm ($2\theta = 45.18$) almost disappears for samples heated at 325°C (for 2 h) and above (Fig. 2).

Besides the presence of NiO and for nickel concentrations greater than 4.6% (as NiO) a band appears at a d distance of 0.202 nm for samples heated at 225°C and is shifted to 0.2034 nm for heat treatment at 700°C. Samples heated at temperatures above 500°C do not produce any further structural changes except

that the boehmite of the support changes to $\gamma\text{-Al}_2\text{O}_3$. By comparison with our previous work carried on the adsorption of copper [27] and nickel amine complexes [17] on amorphous silica support, two characteristic bands of a surface compound appeared in each case, these are at d distances of 0.203 to 0.233 nm and

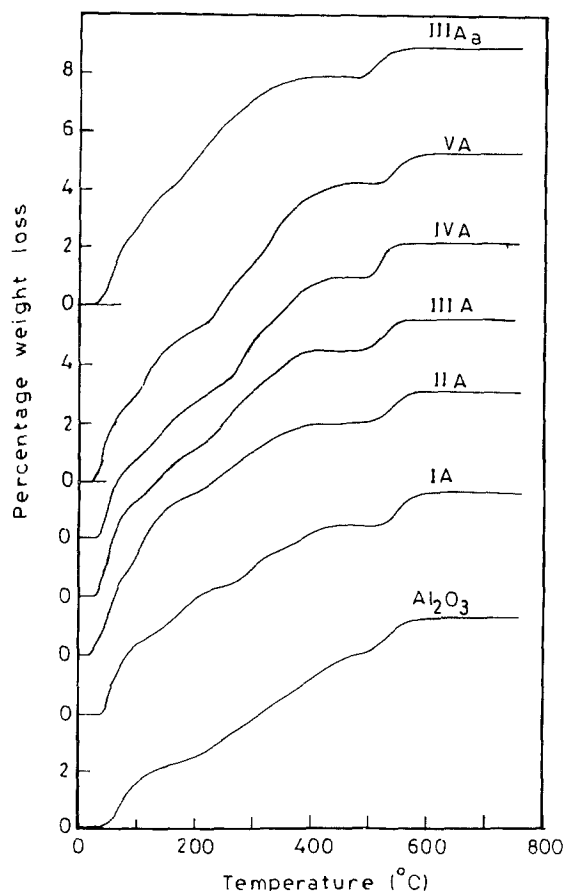


Figure 3 Thermogravimetric curves for catalyst samples IA-VA, IIIAa and Al_2O_3 (soaked in H_2O).

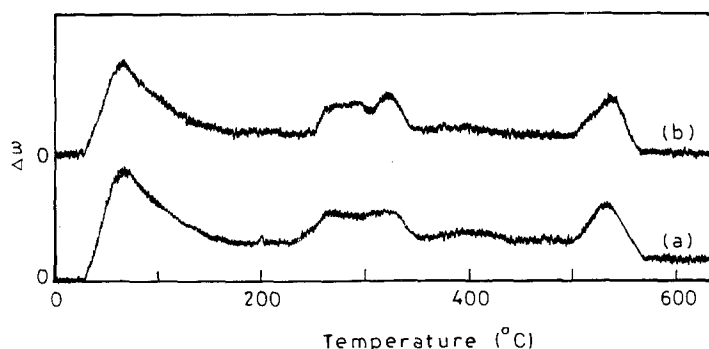
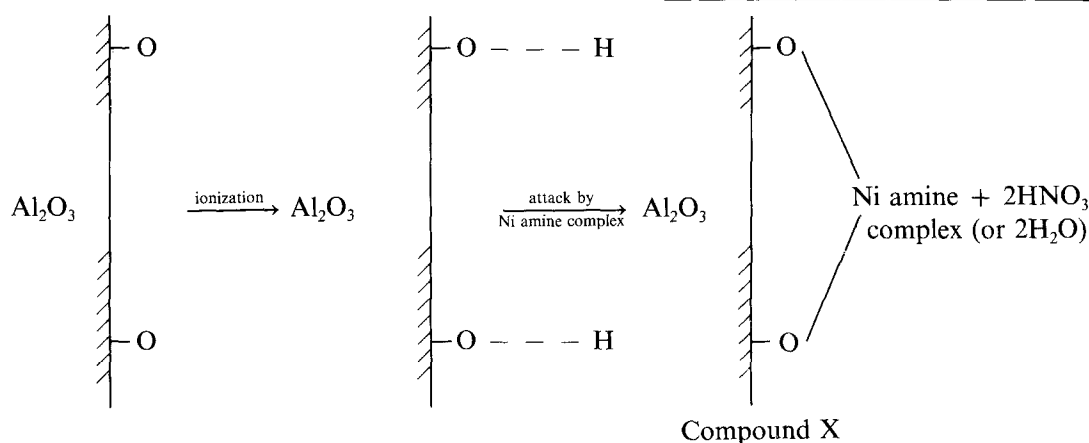


Figure 4 Differential thermogravimetric analysis curves for catalyst samples (a) IIA and (b) VA.

0.2035 to 0.2349 nm, respectively. By analogy with our present surface species, together with the band observed in the range 0.202 to 0.2034 nm a band at a 2θ range of 44.5 to 44.8° (d -distance of 0.2363 to 0.2348 nm) should also be present. This is actually so being more distinct for the high temperature treated samples since at lower temperatures overlap with the boehmite pattern (peak at d -distance of 0.2343 nm [20]) occurs. Such a surface species is believed to arise from the attack of the amine complex on two adjacent hydroxyl groups on the alumina surface. The alumina surface is known to comprise several differently active surface hydroxyl groups [12]. It thus seems reasonable to assume that the alumina surface is polarized at such high pH medium, similar to silica [28] and since almost similar bands are obtained here, then the scheme given before [17, 27] for the surface attack can be applied here as well



It is worth noting that the nickel amine complex can have as counter ions either the NO_3^- ions or the $(\text{OH})^-$ ions and it appears that both are present. Such a surface structure is thermally stable as a result of its high membered ring (≥ 5) structure [29]. The appearance of these two characteristic X-ray bands of such surface compounds, whether the support is alumina or silica, and whether the supported cation is copper or nickel is now evident. Comparison of the d distances obtained in this investigation (e.g. that of the sample heated at 700°C) with those previously reported for either copper or nickel amine complexes on silica supports shows that the resulting d distances of the formed surface species is the same for the nickel-supported catalysts irrespective of the nature of the support. This might lead us to believe that it has the same ring structure as that on the silica support i.e. it forms a six-membered ring structure.

3.1.2. Thermogravimetric analysis

The TGA samples IA to VA and IIIAa together with the support soaked in water only for an identical time interval are shown in Fig. 3.

The TG curves of the alumina sample soaked in water exhibit three distinct steps; the first resulting from the evolution of physically adsorbed water and covers the temperature range ~ 50 to 150°C .

The second arises from the evolution of constitutional and/or interstitial water and covers a wide temperature range, namely ~ 200 to 460°C . The third and last step is responsible for the dehydroxylation [30] of boehmite to $\gamma\text{-Al}_2\text{O}_3$ as also manifested by X-ray analysis.

The Tg curves of all catalyst samples exhibit several steps of weight losses, the first commencing at $\sim 50^\circ\text{C}$ and terminating at $\sim 100^\circ\text{C}$ overlaps with the second that terminates at a temperature range ~ 200 to

250°C . Estimation of the corresponding percentage weight losses of these two steps show them to be almost constant for samples IIA to VA with an average value of 3.05 and 2.32%, respectively, pointing to their independence of nickel content. Samples IA and IIIAa show a slightly lower value (Table I, columns 3, 4, respectively). The first step is similar to that observed for the support alone and points to the evolution of physically adsorbed water. The slightly increased amount may result from the hydration of the chemisorbed nickel ions. The second step seems to arise from the evolution of physically adsorbed ammonia and not that existing as a ligand [17], whose evolution appears to be associated with the formation of the crystalline surface complex. This step may also include some physically adsorbed water evolved from the support itself. Following these two steps is a third large step terminating at about 450°C and for the

sample with nickel concentration of 13.4% it is found to comprise two steps. The presence of these two steps are manifested in the corresponding DTG curves where two distinct peaks appeared at around 260°C and 325°C for samples with nickel concentrations in excess of 4.6 (% NiO); the former is broad and appears to constitute two processes. Below this concentration these peaks overlap and appear as one broad peak (Fig. 4). The first of these two peaks is believed to result from the decomposition of the physically adsorbed surface species $[\text{Ni}(\text{NH}_3)_6](\text{NO}_3)_2$ as well as from the evolution of the ammonia ligand from both the surface compound X and from the adsorbed species $[\text{Ni}(\text{NH}_3)_6](\text{OH})_2$. The DTG peak centred at about 325°C, appearing immediately after the evolution of the ammonia ligand, results from the dehydroxylation of the resulting $\text{Ni}(\text{OH})_2$ [26]. It is worth noting that the dehydroxylation temperature may be affected by ageing and also by the surrounding conditions of the solid substrate, similar to mixed hydroxides [32]. Included in this temperature range is the evolution of some water from the alumina support itself (compare curve for alumina alone) as well as any chemisorbed NH_3 that is evolved in this temperature range [17].

The last step observed in the TG curves in the temperature range 520 to 560°C and also in the DTG curves (Fig. 4) is unaffected by any change in the nickel content (Table I, column 6) and results from boehmite dehydroxylation.

It is worth noting that sample IIIAa shows a high percentage weight loss for the third step as compared to the corresponding sample IIIA of comparable nickel concentration though the total percentage weight loss is less (Table I, columns 5, 7 resp.). This shows clearly that equilibrium conditions are not actually reached within a soaking period of 7 days. Even the amount of nickel uptake was lower by 0.3% for the sample soaked for 7 days than for that soaked for 15 days though the same concentration of impregnating solution was used.

3.1.3. Differential thermal analysis

The DTA curves of all the catalyst samples exhibit a broad endothermic peak centred at around 95°C (Fig. 5) and covering the same temperature range (50 to 200°C) for the evolution of physically adsorbed H_2O and NH_3 as observed in the TG curves (Fig. 3). This is followed by an exotherm in the temperature range 240 to 270°C with a peak apex and a shoulder. For nickel-concentrations less than 4.6% a peak is observed at around 270°C preceded by a shoulder at around 248°C. For higher nickel concentrations it is observed at around 250°C followed by the shoulder at about 270°C and further increase in nickel concentrations shows this exotherm to trace a broad apex that appears to be interrupted by an endothermic effect. From the IR spectra obtained, free NO_3^- is detected by the presence of a band at 1385 cm^{-1} [33] followed by a small one at 1375 cm^{-1} thus changing from D_{3h} symmetry to a less symmetrical species. No bands are observed for NO_3^- in the inner coordination sphere being a strong oxidizing agent

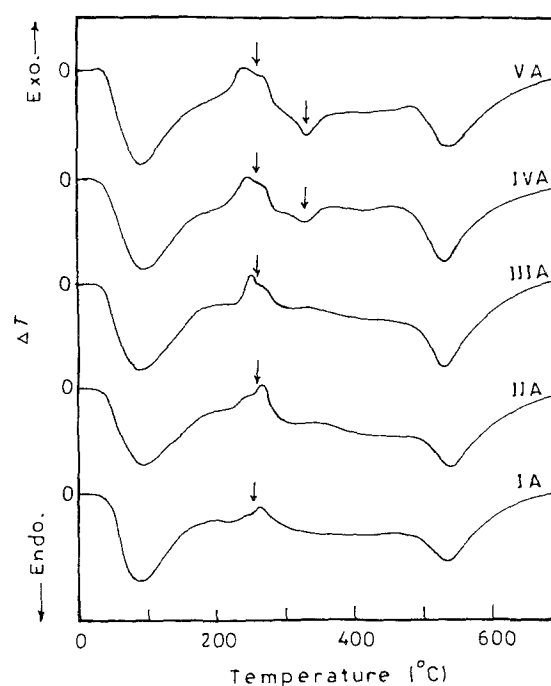


Figure 5 Differential thermal analysis curves for catalyst samples IA-IVA.

[34]. The only plausible explanation is that the decomposition of the surface adsorbed complex species takes place exothermally where the counter ion is a nitrate [35], while the evolution of the ammonia ligands including that of the adsorbed species $[\text{Ni}(\text{NH}_3)_6](\text{OH})_2$ should be endothermic and since both processes take place simultaneously, only the net thermal effect is observed. It is worth noting here that the XRD bands characterizing the presence of the surface nickel compound appeared for samples heated to above 225°C (2h). Whether the crystalline surface aluminate (d distance ~ 0.202 and 0.2348 nm) is formed before or after the evolution of the ammonia ligand is hard to distinguish at present but the stability of this crystalline species at higher temperatures favours its formation after the evolution of the ammonia ligand. At 325°C an endotherm is clearly observed for nickel concentrations of 9.6 and 13.4% being larger for the higher nickel concentration. It appears that for higher nickel concentrations, there is a greater tendency for the species $[\text{Ni}(\text{NH}_3)_6](\text{OH})_2$ to form and upon the evolution of the ammonia ligand $\text{Ni}(\text{OH})_2$ is left behind that decomposes to the oxide at about 325°C as previously discussed (X-ray section).

It is important to recall that differences in the temperature as observed from TG (or DTG) and DTA data arise from the different transfer process in the two techniques.

The last endotherm is observed at a temperature of about 530°C and is unaffected by the concentration of impregnated material resulting from the dehydroxylation [30] of boehmite to $\gamma\text{-Al}_2\text{O}_3$.

3.2. Textural properties

3.2.1. Effect of nickel concentration

Adsorption-desorption isotherms of nickel are obtained at -196°C for all the catalyst samples as well as for the thermally treated products of catalyst

samples IIIA and IIIAa. N₂ isotherms were also obtained for the pure alumina used in this investigation and for the sample soaked in NH₄OH solution for the same time interval and pH as the catalyst samples.

The adsorption isotherm of the pure support is a type II isotherm showing some enhanced adsorption at $P/P_0 > 0.6$. Soaking this alumina in high pH using NH₄OH seems to bring about some widening of the pore system as the amount adsorbed has slightly increased along the whole relative pressure range with an increased enhancement in the relative pressure range of 0.65 to 0.90 imposing a near type IV shape to the isotherm.

All isotherms of the catalyst samples exhibit some enhanced adsorption in the relative pressure range 0.65 to 0.90, reflecting the nature of the support and thus possess a shape near that of type IV. The isotherms obtained for the catalysts and alumina samples all exhibit reversible hysteresis loops closing at a relative pressure range 0.50 to 0.60 and whose shapes indicate a wide variation of pore sizes.

Specific surface areas were derived by applying the Brunauer–Emmett–Teller (BET) method (denoted by S_{BET}) assuming that the nitrogen molecule occupies an average area of 0.162 nm² in the complete monolayer (Table II, column 3).

Pore structure analysis is carried out using the t method of Boer [36, 37]. In these plots the t curves of Mikhail *et al.* [38] are employed which match the corresponding BET C-constants of the samples under test. Agreement between S_t and S_{BET} is observed for all samples thus fulfilling the criteria [39] for computing a correct S_t value (Table II, columns 4 and 3, respectively).

Soaking the alumina support in high pH (~10) produces some widening in the pore system that results in a mild increase in specific surface area,

total pore volume ($V_{\text{P}0.95}$) and average pore radius ($\bar{r}_{\text{H}} = V_{\text{P}0.95}/S_{\text{BET}}$ assuming parallel plate structure). This is in accordance with our previous discussion for the decondensation of alumina at such a high pH due to its atmospheric nature. This is reflected in the corresponding V_1-t plot where not only widening of the pores occurs but also two groups of pore sizes are revealed in the mesopore range. The first of narrower dimension is observed at a t value range 0.370 to 0.60 nm followed by the second group of wider pores (Fig. 6 curve b). This appears to imply the presence of particles (secondary) that are individually made up of smaller particulates (primary).

In the presence of small amounts of nickel (1.5% NiO) the area is found to increase markedly and is accompanied by an increase in total pore volume and a decrease in average pore radius (Table II, columns 3, 5 and 6, respectively). The presence of NiAl₂O₄ on the surface (Section 3.1.1.) could not possibly result in these changes and the reverse would have been expected. The changes observed in the crystallinity of boehmite upon impregnation in the nickel–amine complex seem to be responsible for the resulting textural variation since alterations in the crystallite dimensions is normally reflected on the pore system. This change in the porous texture is clearly reflected in the corresponding V_1-t plot where a marked narrowing of the pore system is observed along the whole relative pressure range (Fig. 6).

An increase in the nickel content up to 3.2% produced a corresponding decrease in S_{BET} and $V_{\text{P}0.95}$ and an increase in \bar{r}_{H} . This resulted from the blocking of the narrower pores by the impregnated nickel leaving behind the wider pores only.

Sample IIIA, with 4.6% (NiO), exhibited a marked decrease in area that is accompanied by widening of the pores, \bar{r}_{H} changing from 3.680 nm (sample IIA) to 4.368 nm, with an increase in the total pore volume.

TABLE II Surface parameters of all the catalyst samples, the thermally treated products of catalysts IIIA and IIIAa together with those of alumina before and after soaking in NH₄OH solution

Sample	BET C-Constant	S_{BET} (m ² g ⁻¹)	S_t (m ² g ⁻¹)	$V_{\text{P}0.95}$ (ml g ⁻¹)	\bar{r}_{H} (nm)
IA	12	167.4	174.0	0.289	1.72
IIA	17	143.0	140.0	0.264	1.84
IIIA	18	125.0	130.0	0.273	2.18
IIIAa	8	161.0	159.0	0.249	1.55
IVA	7	187.0	184.0	0.281	1.50
VA	11	164.0	170.0	0.256	1.56
IIIA-120	19	137.2	137.0	0.237	1.73
IIIA-225	11	120.0	126.0	0.243	2.03
IIIA-325	28	126.0	134.0	0.244	1.94
IIIA-500	14	151.0	150.0	0.289	1.91
IIIA-700	13	134.0	136.0	0.229	1.71
IIIAa-120	8	180.0	178.0	0.293	1.63
IIIAa-225	26	115.0	114.0	0.228	1.98
IIIAa-325	20	137.0	138.0	0.268	1.91
IIIAa-500	15	153.0	156.0	0.278	1.81
IIIAa-700	16	132.9	132.0	0.260	1.96
Al ₂ O ₃ (pure)	30	120.0	121.0	0.235	1.96
Al ₂ O ₃ (soaked in NH ₄ OH)	25	124.7	126.0	0.270	2.16

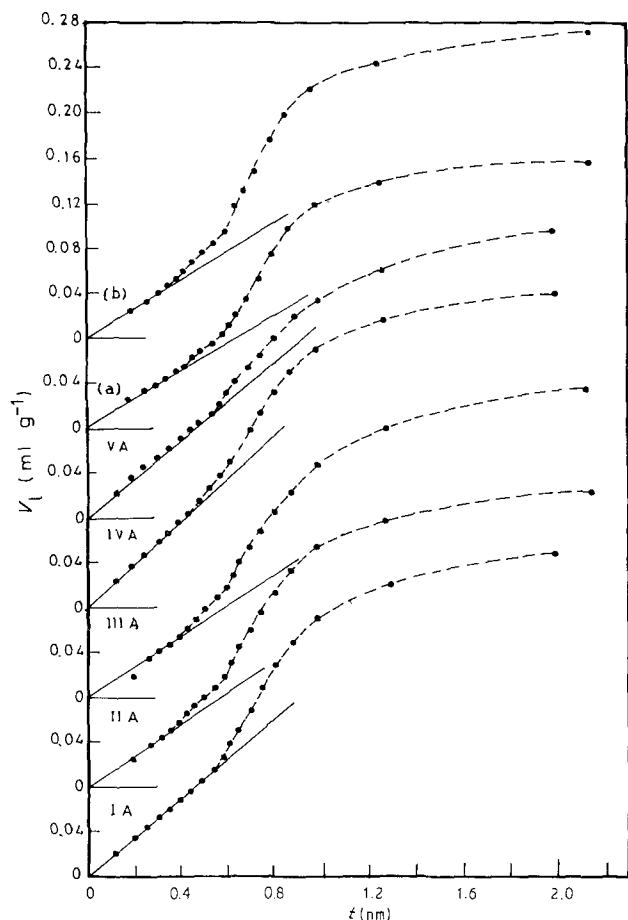


Figure 6 V_t - t plots from nitrogen adsorption on catalyst samples IA-VA, on (a) pure alumina and (b) alumina soaked in NH_4OH .

This can result from a process analogous to the agglomeration of the particles. This is clearly observed in its V_t - t plot that shows a distinct widening in the groups of pores below a t value of 0.6 nm. From XRD data (Section 3.1.1.) a surface compound is found to form—observed upon thermal treatment—for samples with nickel concentrations $> 4.6\%$ and is believed to result from the attack of two adjacent OH

groups. If the OH groups are attached to opposite walls then the formation of such a compound between them may result in the observed textural changes. Increasing the nickel concentration to 9.6% causes a marked increase in area and total pore volume accompanied by a drastic decrease in the average pore radius. This narrowing in the pore system is reflected in the corresponding V_t - t plot (Fig. 6). Such a change may result either from the penetration of the nickel between the alumina particulates (primary particles) thereby creating new pores and affecting the size of the pores between the secondary particles or that the texture of the new surface compound imposes these changes, being more concentrated than in sample IIIA. The former speculation is believed to represent the actual situation as increasing the nickel concentration to 13.6% does not favour a further change in these surface parameters as demanded by the second speculation, but rather produced a decrease in specific surface area and pore volume. This occurred as a result of blocking some of the pores with increase in the nickel concentration to 13.6%. From the V_t - t curve it can be seen that the points fall on the straight line passing through the origin up to a t value of 0.6 nm for sample VA whereas an upward deviation is observed at a t value of about 0.42 nm for sample IVA.

3.2.2. Effect of impregnation period on the thermal products

The role of the period of impregnation on the texture of the catalyst samples was investigated for a nickel concentration in the range 4 to 5%. Thus sample IIIAa obtained by soaking the alumina in the nickel amine solution for 7 days was found to possess a higher specific surface area than the corresponding sample IIIA soaked for 15 days approaching that possessed by sample IA with the concentration of 1.5% (NiO) (Table II, column 3). It also possessed a narrower pore system reflected in the values of \bar{r}_H and $V_{P0.95}$ as compared to those of sample IIIA. Such

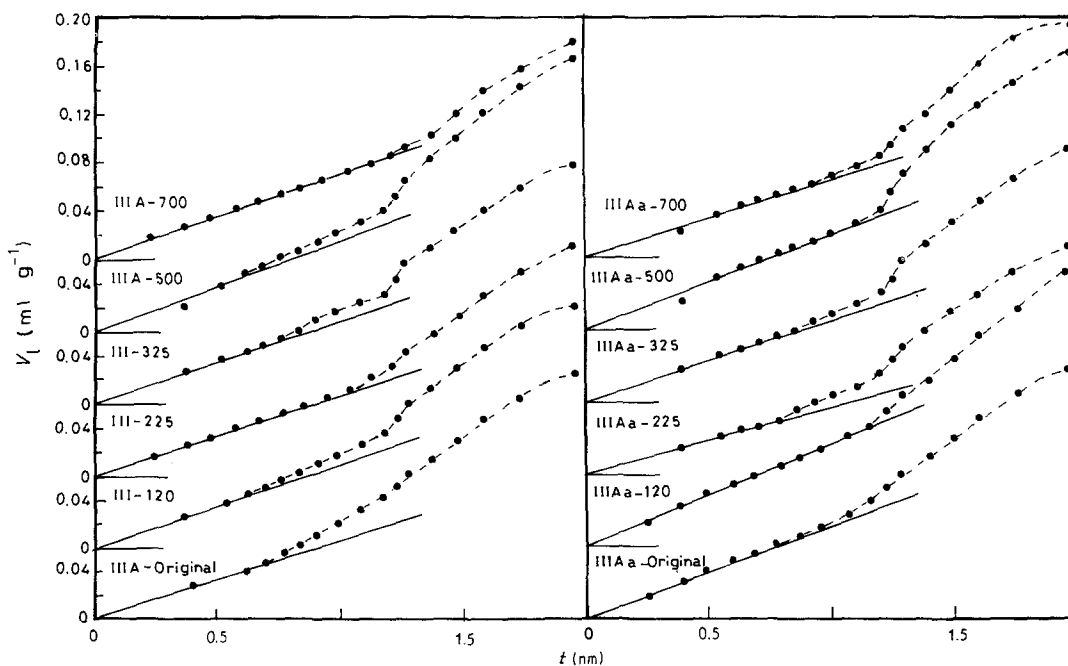


Figure 7 V_t - t plots from nitrogen adsorption on catalyst samples IIIA and IIIAa and their products of thermal treatment.

changes in the pore structure were also observed in their corresponding V_1-t plots (Fig. 7). Sample IIIA exhibited an upward deviation at a t value of about 0.37 nm being enhanced above a thickness of about 0.60 nm thereby exhibiting two groups of mesopores whereas sample IIIAa showed an upward deviation above a t value of about 0.55 nm where only one group of mesopores could be detected and which is similar to that of sample IA (1.5% Ni). Such differences in surface parameters are expected when the extent of the various physical and/or chemical interactions of the impregnating cations with the support is different. In fact from TG data (Table I, also Section 3.1.2.) it was clear that soaking for 7 days actually represented the non-regular equilibrium state. To what extent such a non-equilibrium situation of cation uptake affects the texture of the corresponding thermally treated products is visualized from the surface parameters given in Table II for samples IIIA and IIIAa heated to the same temperature except for the specific area which is unaffected by soaking period for temperatures above 500°C. Nevertheless, even at such a high temperature as 700°C, for example, the total pore volume and the average pore radius are higher for sample IIIAa of lower soaking period.

The variations in pore structure as revealed by their V_1-t plots emphasize the lack of any common trend. Thus, though products of sample IIIA show the existence of two groups of mesopores for the original sample and those samples heated at 120, 325 and 500°C, sample IIIAa shows them for products obtained at 225 and 325°C only.

References

1. K. MORIKAWA, T. SHIRASAKI and M. OKADA, in "Advances in Catalysis" edited by D. D. Eley, H. Pines and P. B. Weisz, Vol. 20 (Academic Press, New York, 1968) p. 97.
2. I. FURUOYA and T. SHIRASAKI, *Bull. J. Petrol. Inst.* **13** (1971) 78.
3. F. BASOLO and R. L. BURWELL, Jr., "Catalysis Progress in Research" (Plenum, New York, 1973)
4. M. LO JACONO and M. SCHIAVELLO, in "Preparation of Catalysis" edited by B. Delmon, P. A. Jacobs and J. Poncelet (Elsevier, Amsterdam, 1976) p. 473.
5. F. BOZON-VERDURAZ, M. TARDY, G. BUGLI and G. PAMELIA, in "Preparation of Catalysis" edited by B. Delmon, P. A. Jacobs and J. Poncelet (Elsevier, Amsterdam, 1976) p. 266.
6. E. G. DEROUANE, J. B. NAGY and J. C. VERDRUIE, *J. Catal.* **46** (1977) 434-7.
7. T. HIDEMITSU, O. YOSHIO and K. TOMINAGA, *ibid.* **40** (1975) 197-202.
8. B. SAMANOS, P. BOUTRY and R. MONTARNAL, *C. R. Acad. Sci. C* **247** (1972) 575.
9. J. K. GIMZEUSKI, T. DONNELLY and S. AFFROSSMOU, *J. Catal.* **47** (1977) 78-84.
10. J. T. RICHARDSON, *ibid.* **21** (1971) 122.
11. H. HONL and W. STUMM, *J. Colloid Interface Sci.* **55** (1976) 281-8.
12. J. B. PERI, *J. Phys. Chem.* **69** (1965) 211-220.
13. M. P. ROSYNEK, W. D. SMITH and J. W. HIGHTOWER, *J. Catal.* **23** (1971) 204.
14. P. C. SAUNDERS and J. W. HIGHTOWER, *J. Phys. Chem.* **74** (1970) 4323.
15. S. P. AHUJA, M. L. DERRIEU and J. F. Le PAGE, *Ind. Eng. Chem. Prod. Res. Dev.* **9** (1970) 272.
16. V. H. T. De BEER, PhD Thesis, Eindhoven, University of Technology, The Netherlands (1975).
17. S. HANAFI, A. AMIN, S. M. SOLIMAN and S. A. SELIM, *Thermochimica Acta*, **95** (1985) 159-178.
18. J. V. SMITH, (Ed.), "X-Ray Powder Data File and Index to X-Ray Data File" (American Society for Testing and Materials, Philadelphia, 1961).
19. Powder Diffraction File, ASTM Alphabetical Index of Inorganic Compounds, Published by the International Center for Diffraction Data, 1978, Swathmore, PA 19081, USA.
20. B. C. LIPPENS and J. J. STEGGERDA, in "Physical and Chemical Aspects of Adsorbents and Catalysis" edited by B. G. Linsen.
21. N. N. GREENWOOD and A. EARNSHAW, in "Chemistry of the Elements" (Pergamon, Oxford 1984).
22. M. LO JACONO, A. CIMINO and G. C. A. SCHNIT, *Gazz. Chim. Ital.* **103** (1973) 1281.
23. E. J. W. VERENEY, *Z. Kristallgr.* **91** (1935) 317.
24. H. JAZODSZINSHI and H. SAALFELD, *Ibid.* **110** (1958) 197.
25. H. SAALFELD, *News Jb. Miner. Abh.* **95** (1960) 1.
26. J. J. B. VAN VOORTHUYSEN, E. VAN and P. FRANZEN, *Recl. Trav. Chim. Pays-Bas*, **70** (1951) 793-812.
27. S. A. SELIM, H. A. HASSAN, M. ABD-EL KHALIL and R. SH. MIKHAIL, *Thermochimica Acta* **45** (1981) 349-360.
28. J. P. BRUNELLE, *Pure Appl. Chem.* **50** (1978) 9.
29. D. DOLLIMORE and R. C. MAKENZIE (Eds), "Differential Thermal Analysis" Vol I (Academic, London, 1970) p. 443.
30. R. C. MAKENZIE, in "The Differential Thermal Investigation of Clays" edited by R. C. Makenzie (Mineralogical Society, London, 1957) pp 299-328.
31. V. P. CHALYI, O. I. SHOR and S. P. ROZHENKO, *Ukr. Khim. Zh.* **27** (1961) 3-6.
32. V. P. CHALYI and O. I. SHOR, *ibid.* **27** (1961) 7-11.
33. F. A. COTTON and G. WILKINSON, (Eds) "Advanced Inorganic Chemistry" 3rd edn. (Interscience Publishers, New York, 1972) p. 64.
34. W. W. WENDLANT and J. L. BEAR, *J. Phys. Chem.*, **65** (1961) 1516-1519.
35. W. W. WENDLANT, *J. Inorg. Nucl. Chem.*, **25** (1963) 545-551.
36. B. C. LIPPENS, B. G. LINSEN and J. H. De BOER, *J. Catal.*, **3** (1964) 32.
37. J. H. De BOER, B. G. LINSEN and Jh. J. OSINGA, *ibid.* **4** (1965) 643.
38. R. Sh. MIKHAIL, N. M. GUINDY and S. HANAFI, *Egypt J. Chem. Special Issue "Tourky"* **53** (1973).
39. R. Sh. MIKHAIL and F. SHEBL, *J. Colloid Interface Sci.*, **34** (1970) 65.

Received 26 September 1988
and accepted 13 February 1989